American Journal of Pathology, Vol. 166, No. 6, June 2005

Vascular Biology, Atherosclerosis and Endothelium Biology

Anthrax Lethal Toxin Induces Endothelial Barrier Dysfunction

Jason M. Warfel, Amber D. Steele, and Felice D'Agnillo

From the Laboratory of Biochemistry and Vascular Biology, Division of Hematology, Center for Biologics Evaluation and Research, Food and Drug Administration, Bethesda, Maryland

Hemorrhage and pleural effusion are prominent pathological features of systemic anthrax infection. We examined the effect of anthrax lethal toxin (LT), a major virulence factor of *Bacillus anthracis*, on the barrier function of primary human lung microvascular endothelial cells. We also examined the distribution patterns of cytoskeletal actin and vascular endothelial-cadherin (VE-cadherin), both of which are involved in barrier function regulation. Endothelial monolayers cultured on porous membrane inserts were treated with the LT components lethal factor (LF) and protective antigen (PA) individually, or in combination. LT induced a concentration- and time-dependent decrease in transendothelial electrical resistance that correlated with increased permeability to fluorescently labeled albumin. LT also produced a marked increase in central actin stress fibers and significantly altered VE-cadherin distribution as revealed by immunofluorescence microscopy and cell surface enzyme-linked immunosorbent assay. Treatment with LF, PA, or the combination of an inactive LF mutant and PA did not alter barrier function or the distribution of actin or VE-cadherin. LT-induced barrier dysfunction was not dependent on endothelial apoptosis or necrosis. The present findings support a possible role for LT-induced barrier dysfunction in the vascular permeability changes accompanying systemic anthrax infection. *(Am J Pathol 2005, 166:1871–1881)*

Bacillus anthracis, the causative agent of anthrax, is a spore-forming gram-positive bacterium. Anthrax toxin, the major virulence factor of *B. anthracis*, is composed of three proteins: protective antigen (PA), lethal factor (LF), and edema factor (EF). PA and LF combine to form lethal toxin (LT), and EF combines with PA to form edema toxin (ET).[1–3] PA binds at least two identified cell surface receptors, tumor endothelial marker 8 and capillary morphogenesis protein 2.[2,4,5] Once formed, PA-receptor complexes facilitate the endocytosis of LF and EF. Inside cells, LF acts as a metalloprotease that cleaves all of the mitogen activated protein kinase kinases (MEKs) except MEK 5, thus disrupting the activation of major mitogen-activated protein kinases (MAPKs): extracellular signal-regulated kinases 1 and 2 (ERK1/2), p38 MAPK, and c-Jun NH_2-terminal kinases (JNK).[6–8] EF acts as a Ca^{2+}/calmodulin-dependent adenylate cyclase that causes a dramatic increase in intracellular levels of cAMP.[9,10] Evidence to date suggests that LT may play a more significant role than ET in the pathogenesis of systemic anthrax. In several animal models, intravascular injections of purified LT are lethal.[11–13] In addition, attenuated *B. anthracis* strains unable to produce functional LF are 1000-fold less virulent than normal strains, whereas EF-lacking strains are 10-fold less virulent.[14]

Vascular dysfunction or injury has long been considered a hallmark of anthrax pathogenesis.[15–17] Prominent pathological features of systemic anthrax infection include vascular leakage, hemorrhages, and vasculitis. Guarner et al[18] reported progressive and persistent pleural effusions as the main feature in inhalational anthrax patients from the 2001 bioterrorism attack in the United States. During the 1957 inhalational anthrax epidemic in

Supported by the National Institute of Allergy and Infectious Diseases, National Institutes of Health (Biodefense Research grant to F.D.); this grant also supported the postgraduate research program appointment of A.D.S. at the Center for Biologics Evaluation and Research from the Oak Ridge Institute for Science and Education through an interagency agreement between the U.S. Department of Energy and the U.S. Food and Drug Administration. Supported in part by the Research Fellowship Program for the Center for Biologics Evaluation and Research from Oak Ridge Associated Universities and the U.S. Food and Drug Administration (to J.M.W.).

Accepted for publication February 15, 2005.

The opinions and assertions contained herein are the scientific views of the authors and are not to be construed as policy of the United States Food and Drug Administration.

Address reprint requests to Felice D'Agnillo, Ph.D., Center for Biologics Evaluation and Research, Food and Drug Administration, 29 Lincoln Drive, Bldg. 29, Rm. 129, Bethesda, MD 20892. E-mail: dagnillo@cber.fda.gov.

New Hampshire, autopsies consistently showed edema, pleural effusion, and hemorrhages.[19] Grinberg et al[20] described high-pressure and low-pressure hemorrhages, particularly in the lungs and spleens, in the inhalational anthrax victims of the Sverdlovsk incident. Rhesus and cynomolgus monkeys exposed to the fully virulent Ames strain showed edema, hemorrhages, and a variable degree of leukocyte infiltration in various tissues.[21,22] Similar findings have recently been described in anthrax-infected wild chimpanzees.[23]

Studies in mice and rats have shown that administration of purified LT, in addition to causing death, produces vascular leakage similar to that observed in systemic anthrax.[11,12] Although these studies support a causative role for LT in the vascular leakage pathology of anthrax, the specific events or mechanisms are not known. Vascular endothelium, which plays a central role in regulating vascular permeability, is a likely target for LT during systemic anthrax infection by virtue of its direct contact with the bloodstream. In the present study, we examined the effects of LT on endothelial barrier function using cultured primary human lung microvascular endothelial cells. The effects of LT on the cellular distribution and expression of cytoskeletal actin and vascular endothelial-cadherin (VE-cadherin) were also investigated. VE-cadherin, the major component of adherens junctions (AJs), plays a key role in regulating endothelial barrier function as evidenced by the increased permeability caused by the disruption of interendothelial AJs both *in vitro* and *in vivo*.[24–28] In addition, actin reorganization has been associated with compromised barrier integrity and the creation of interendothelial gaps.[26] In the present study, we report that LT causes endothelial barrier dysfunction *in vitro*, supporting a potential role for LT in the vascular permeability changes accompanying systemic anthrax infection.

Materials and Methods

Materials

Phosphate-buffered saline (PBS), Hank's balanced salt solutions with calcium and magnesium ($HBSS^+$) or without ($HBSS^-$), and L-alanyl-L-glutamine (GlutaMAX I) were obtained from Invitrogen (Carlsbad, CA). Bovine serum albumin (BSA), propidium iodide (PI), Triton X-100, Hoechst 33342, and fluorescein isothiocyanate-labeled human serum albumin (FITC-HSA) were obtained from Sigma Chemical Co. (St. Louis, MO). Enzyme-linked immunosorbent assay (ELISA) detection reagents (hydrogen peroxide and 3,3′,5,5′ tetramethylbenzidine), FITC-labeled annexin V and a mouse IgG1 primary monoclonal antibody that binds to the extracellular domain of VE-cadherin were purchased from BD Biosciences (San Diego, CA). Alexa Fluor 555-labeled goat anti-mouse IgG1 secondary antibody and Alexa Fluor 488-labeled phalloidin were purchased from Molecular Probes (Eugene, OR). Peroxidase-conjugated goat anti-mouse IgG (H+L) secondary antibody was obtained from Jackson ImmunoResearch (West Grove, PA). U0126, an inhibitor of MEK1/2; SB230580, an inhibitor of p38 MAPK; and SP600125 (JNK inhibitor II), an inhibitor of JNK, were purchased from CalBiochem (San Diego, CA). Caspase inhibitor, z-VAD-fmk (zVAD), was obtained from Enzyme Systems Products (Livermore, CA). LF, PA, and mutant LF_{E687C} were prepared as previously described and kindly provided by Dr. Stephen H. Leppla (National Institutes of Health, Bethesda, MD).[29,30] Toxin proteins were diluted in sterile PBS before cell treatment.

Endothelial Cell Culture

Primary human lung microvascular endothelial cells were obtained from Cambrex (Walkersville, MD). Cells were grown in phenol red-free MCDB 131 medium (Hyclone, Logan, UT) supplemented with 10 mmol/L L-alanyl-L-glutamine, human epidermal growth factor, hydrocortisone, gentamicin, amphotericin-B, vascular endothelial growth factor, human fetal growth factor-B, recombinant growth factor-1 (R^3-IGF-1), ascorbic acid, and 5% fetal bovine serum (Cambrex). Cells were cultured in 100-mm dishes at 37°C in a humidified atmosphere of 95% air and 5% CO_2. Cells were passaged 1:3 when cultures reached 90 to 95% confluence. For harvesting, cells were washed with HEPES-buffered saline and incubated with 0.025% trypsin/0.01% EDTA for 7 minutes at 37°C. After cell detachment, trypsin-neutralizing agent was added, and cells were centrifuged at 220 × *g* for 5 minutes at 4°C. Cell counts were obtained using a Z1 dual threshold Coulter counter (Beckman-Coulter, Hileah, FL). Experimental data were obtained from cells in their third to seventh passages.

Transendothelial Electrical Resistance (TEER) Measurement

Cells were grown to confluence on porous polyester membrane inserts (12 mm diameter, 0.4 μm pore size; Transwell, Corning, Cambridge, MA). The upper and lower compartments contained 0.5 and 1.5 ml of media, respectively. For experimental treatments, LF (1 to 1000 ng/ml), PA (1 to 1000 ng/ml), or both (LT) were added to the upper compartment. Alternatively, catalytically inactive mutant LF_{E687C} (1 μg/ml) was added in the presence of 1 μg/ml PA. TEER measurements were performed using an EVOM volt-ohmmeter connected to a 12-mm Endohm unit (World Precision Instruments, Sarasota, FL). To measure TEER, culture inserts were transferred to the Endohm chamber containing 1.8 ml of $HBSS^+$. The Endohm unit was washed with sterile PBS between measurements to avoid treatment cross-contamination. At the indicated time intervals, resistance readings (ohms) were obtained from each insert and multiplied by the membrane area (ohms × square centimeters). The resistance value of an empty culture insert (no cells) was subtracted. A decrease in TEER indicates an increase in monolayer permeability, whereas an increase in TEER signifies an increase in monolayer integrity. Data were collected from duplicate inserts per treatment in each experiment. Values were reported as the percentage of basal TEER obtained by dividing the resistance values of each

treated monolayer by the resistance value of the control monolayer at each given time point.

Albumin Permeability Assay

Cells grown to confluence on porous membrane inserts (12 mm diameter, 0.4 μm pore size) were treated as described in the previous section. After 72 hours, 50 μl of culture medium from the upper chamber was replaced with an equal amount of medium containing 5 mg/ml FITC-HSA (final concentration 500 μg/ml). After 2 hours, 20 μl samples were drawn from the lower chamber and diluted 10-fold. Data were collected from duplicate inserts per treatment in each experiment. Fluorescence measurements were obtained using a microplate reader (Genios, Tecan, Research Triangle Park, NC) with excitation and emission filters of 485 and 535 nm, respectively. FITC-HSA concentrations were calculated using a FITC-HSA standard curve. To quantify the *trans*-membrane flux (micrograms per hour per square centimeter), the FITC-HSA concentration was multiplied by the volume of the lower chamber and divided by the membrane area and the FITC-HSA incubation time.

Immunofluorescence Microscopy

Cells grown to confluence in 24-well dishes were treated with LF, PA, or both (LT). After treatment, the monolayers were washed once with fully supplemented media containing 5% fetal bovine serum and then fixed with 3.2% paraformaldehyde (Electron Microscopy Sciences, Ft. Washington, PA) for 10 minutes. The cells were then washed twice with $HBSS^+$ supplemented with 0.1% BSA and permeabilized with 0.1% Triton X-100 for 5 minutes. After two washes with 0.1% BSA, the cells were incubated for 1 hour with a primary monoclonal antibody to VE-cadherin (1 μg/ml, 1:200). The cells were then washed twice with 0.1% BSA and subsequently incubated for 1 hour with an Alexa Fluor 555-labeled secondary antibody (2 μg/ml, 1:800). Forty minutes into the second incubation, Alexa Fluor 488-labeled phalloidin (0.2 μg/ml) was added to stain F-actin, and Hoechst 33342 (10 μg/ml) was added to visualize the nuclei. All incubations were done at room temperature. After staining, the cells were washed three times with 0.1% BSA. Photomicrographs were obtained using an Olympus IX71 inverted microscope (Olympus America, Melville, NY) equipped with an Olympus DP70 digital camera connected to a Pentium 4 computer. Excitation light from the mercury arc lamp was passed through a triple band filter set (U-M61000v2; Chroma Technology Corp., Brattleboro, VT) to capture all three fluorochromes simultaneously or through a second filter set (41002C) for VE-cadherin alone. Standardized microscope and software settings were applied during image capture and postprocessing.

VE-Cadherin Cell Surface ELISA

Cells grown to confluence in 24-well dishes were treated with LF, PA, or both (LT). After treatment, the monolayers were washed once with fully supplemented media containing 5% fetal bovine serum and then fixed with 1% paraformaldehyde in $HBSS^+$ for 20 minutes. After two washes with $HBSS^+$ supplemented with 0.1% BSA, the cells were incubated for 1 hour with the primary monoclonal VE-cadherin antibody (1 μg/ml, 1:200). The cells were then washed three times with 0.1% BSA and incubated for 1 hour with a peroxidase-conjugated secondary antibody (1:10,000 dilution). The monolayers were then rinsed four times with 0.1% BSA, followed by one wash with $HBSS^+$. For detection, equal parts of the substrate reagents hydrogen peroxide and 3,3′,5,5′ tetramethylbenzidine were added to each well. After color development, 1 N HCl was added to stop the reaction. Absorbance was measured at 450 nm using the previously described microplate reader.

Analysis of Monolayer Cell Density

Monolayer cell density was assessed by counting the number of adherent cells with normal nuclear morphology identified by dual staining with the membrane-permeable DNA fluorochrome Hoechst 33342 and PI. This staining method distinguishes between normal, apoptotic, or necrotic cells. Normal cells were defined as those with no PI staining and without evidence of nuclear condensation. Apoptotic cells were defined as those with condensed or fragmented nuclei without PI staining. Necrotic cells were defined as those visibly stained by PI indicative of cell membrane lysis. Briefly, cells grown in 12- or 24-well dishes were treated with varying concentrations of LF (1 to 1000 ng/ml), 1 μg/ml PA, or both (LT). At the indicated time intervals, cultures were incubated with 1 μg/ml Hoechst 33342 and 1 μg/ml PI. After a 20-minute incubation, monolayers were washed once with complete medium. Photomicrographs of five separate fields per well (top, bottom, right, left, and center) were obtained using the microscope and digital camera system described above. Digital images were analyzed using the ImageJ software (National Institutes of Health, Bethesda, MD). For each experiment, monolayer density was calculated as the percentage of adherent cells with normal nuclear morphology relative to untreated cultures performed in parallel.

Annexin V/Propidium Iodide Assay

Cells grown to confluence in 12-well dishes were treated with varying concentrations of LF (1 to 1000 ng/ml), PA (1 μg/ml), or both (LT). Nonadherent and adherent cells, harvested by trypsinization, were pooled, washed twice in $HBSS^-$, and resuspended in 150 μl of assay buffer containing 10 mmol/L HEPES/NaOH, 140 mmol/L NaCl, and 2.5 mmol/L $CaCl_2$, pH 7.4. Annexin V-FITC (5 μl of 2 μg/ml) and PI (10 μl of 5 μg/ml) were added to a 100-μl aliquot of this cell suspension. After a 15-minute incuba-

tion in the dark at room temperature, stained cells were diluted with 200 μl of assay buffer and analyzed using a FACScan flow cytometer (Becton Dickinson Biosciences, San Jose, CA). Data were analyzed from a minimum of 10,000 cells per sample using WinMDI software (version 2.8). Cells stained annexin V positive and PI negative (annexin V+, PI−) were defined as early apoptotic cells. Cells stained annexin V positive and PI positive (annexin V+, PI+) represented late apoptotic or necrotic cells and included any cells damaged nonspecifically during the harvesting procedure.

Cell Redox Activity

Cell redox activity was assessed using the 3-(4,5-dimethylthiazol-2-yl)-5-(3-carboxymethoxy-phenyl)-2-(4-sulfophenyl)-2H-tetrazolium (MTS)-based colorimetric assay (CellTiter 96, AQ_{ueous} One Solution Reagent; Promega, Mannheim, Germany). The MTS reagent is bioreduced mainly by mitochondrial enzymes and electron carriers present in metabolically active cells. Briefly, confluent cultures grown in 96-well dishes were treated with 200 μl of medium alone or medium containing LF (1 to 1000 ng/ml), 1 μg/ml PA, or both (LT). At the indicated time intervals, treatment medium was replaced with 200 μl of phenol red-free MCDB 131 medium supplemented with 10 mmol/L L-alanyl-L-glutamine and 0.1% BSA containing 10 μl of MTS reagent. After a 2-hour incubation, absorbance was read at 492 nm using the previously described microplate reader. Background absorbance readings generated in cell-free wells containing medium and MTS were subtracted from experimental readings. Experiments were run in triplicate or quadruplicate per treatment, and values were reported as the percent MTS reduction relative to untreated wells.

Statistical Analysis

Data are represented as means ± SE for replicate experiments. Statistical analysis was performed by the unpaired two-tailed Student's *t*-test using the JMP (v. 5.1) software (SAS Institute Inc, Cary, NC). $P < 0.05$ was considered statistically significant.

Results

LT Increases Endothelial Monolayer Permeability

The barrier function of endothelial monolayers grown on porous membrane inserts was assessed by the measurement of TEER and the permeability to FITC-HSA. TEER readings were obtained between 0 and 72 hours from monolayers treated with LF, PA, or both (LT). Figure 1 shows that LT produced a progressive decrease in TEER, with statistically significant differences at 12, 24, 48, and 72 hours. LF or PA alone did not produce any changes in TEER. To further assess endothelial barrier sensitivity to LT, monolayers were treated with varying concentrations of either LF or PA in the presence of 1 μg/ml PA or LF, respectively. After 72 hours, a significant decrease in

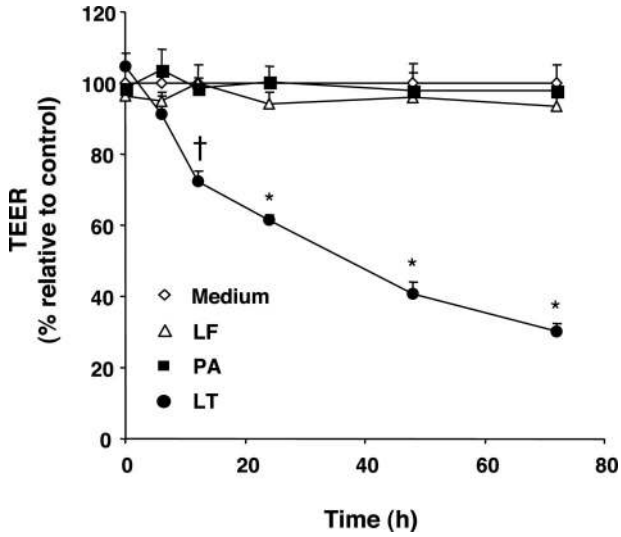

Figure 1. LT induces time-dependent reduction in TEER. Monolayers grown on porous membrane inserts were incubated with medium alone or medium containing 1 μg/ml LF, 1 μg/ml PA, or both (LT). At the indicated time points, TEER readings were obtained as described in Materials and Methods. Values were reported as the percentage of basal TEER obtained by dividing the resistance values of each treated monolayer by the resistance value of the control monolayer at each given time point. The means ± SE for a minimum of three independent experiments are shown ($n = 3$–8). $^{*}P < 0.001$, $^{\dagger}P < 0.05$ versus medium alone.

TEER was measured in cultures treated with 1, 10, 100, and 1000 ng/ml LF (Figure 2A). In PA dose-range experiments, a statistically significant reduction in TEER was observed with ≥10 ng/ml PA (Figure 2B). To determine whether the changes in TEER correlated with an increase in permeability to macromolecules, the flux of FITC-HSA across monolayers was also analyzed. Figure 3A shows that LF concentrations ranging from 1 to 1000 ng/ml in the presence of 1 μg/ml PA enhanced permeability to FITC-HSA. In PA dose-range experiments, significant increases in permeability were observed with PA concentrations ≥100 ng/ml in the presence of 1 μg/ml LF (Figure 3B). The minor increase with 10 ng/ml PA did not reach statistical significance. LF or PA alone did not alter permeability to FITC-HSA (Figure 3, A and B). Moreover, cultures treated with a catalytically inactive mutant LF_{E687C} and PA did not alter TEER or FITC-HSA permeability, indicating that LT-induced barrier dysfunction was dependent on enzymatically active LF (Figures 2A and 3A). Taken together, these two established indices of barrier function provide direct evidence that LT causes endothelial barrier dysfunction *in vitro*.

LT Induces Elongated Morphology, Actin Stress Fiber Formation, and VE-Cadherin Redistribution

To assess whether LT-induced barrier dysfunction correlated with changes in endothelial cell morphology, cultures were examined by phase contrast and immunofluorescence microscopy. LF- or PA-treated monolayers were morphologically indistinguishable from control cultures (Figure 4). LT-treated monolayers remained essentially intact relative to untreated monolayers despite a slight LT-induced elevation in the nonad-

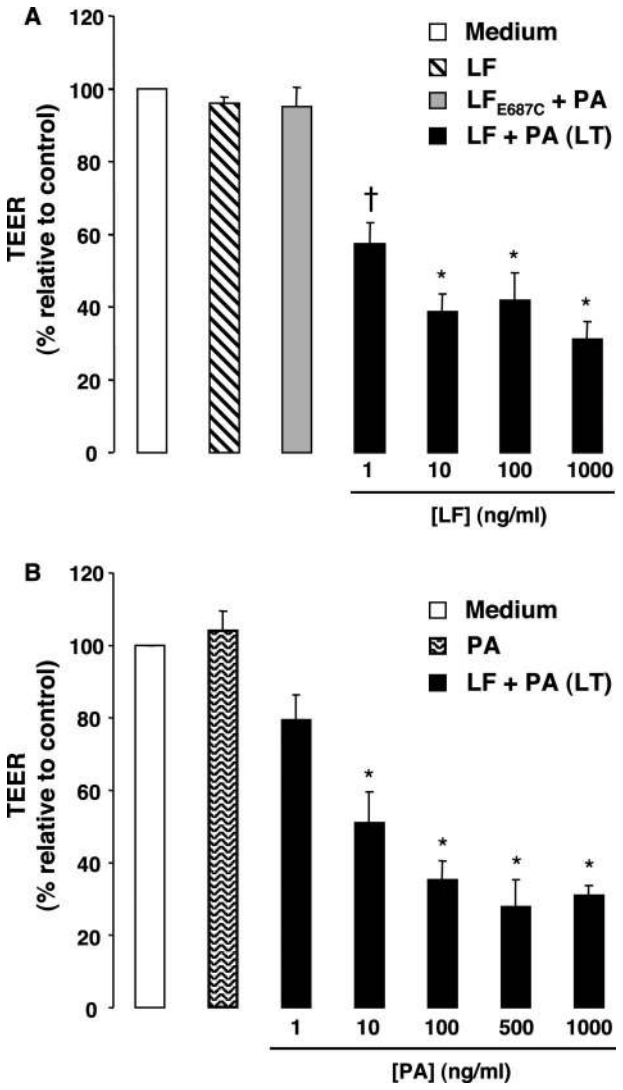

Figure 2. Concentration-dependent effects of LT on TEER. **A:** Monolayers grown on porous membrane inserts were incubated with medium alone or medium containing 1 μg/ml LF, 1 μg/ml LF_{E687C} and PA, or varying amounts of LF in the presence of 1 μg/ml PA. TEER readings were obtained after 72 hours and reported as the means ± SE for a minimum of three independent experiments. $^{*}P < 0.001$, $^{\dagger}P < 0.01$ versus medium alone. **B:** Monolayers were treated with medium alone, medium containing 1 μg/ml PA, or varying amounts of PA in the presence of 1 μg/ml LF. TEER readings were obtained after 72 hours and reported as the means ± SE for a minimum of three independent experiments. $^{*}P < 0.001$ versus medium alone.

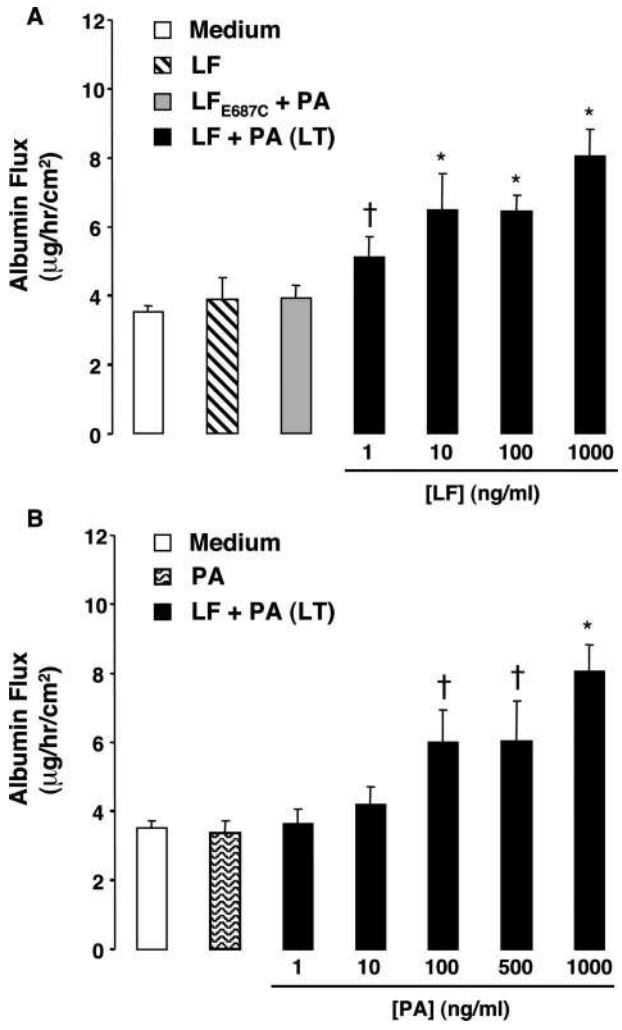

Figure 3. Concentration-dependent effects of LT on albumin permeability. **A:** Monolayers were grown and treated as in Figure 2A. After 72 hours, FITC-HSA was added to the upper compartment of the insert. After 2 hours, the amount of FITC-HSA in the bottom compartment was measured using a fluorescent microplate reader. Values were calculated as the micrograms of FITC-HSA per hour per square centimeter and reported as the means ± SE for a minimum of three independent experiments. $^{*}P < 0.001$, $^{\dagger}P < 0.01$ versus medium alone. **B:** Monolayers were grown and treated as in Figure 2B. Data were collected as in Figure 3A and reported as the means ± SE for a minimum of three independent experiments. $^{*}P < 0.001$, $^{\dagger}P < 0.01$ versus medium alone.

herent cell population over the course of 72 hours. Notably, LT-treated cells exhibited an elongated morphology compared with untreated cells (Figure 4J). This elongated morphology was observed in random regions of the monolayer by 24 hours and became progressively more evident thereafter. By 48 and 72 hours, LT-treated monolayers also contained small interendothelial gaps detectable under high-power magnification (Figure 4J).

To further explore these morphological alterations in the context of barrier function, immunofluorescence staining for filamentous actin (F-actin) and VE-cadherin was performed. Untreated, LF-, or PA-treated monolayers showed strong intercellular connections with F-actin arranged primarily at the periphery, in close association with intense junctional VE-cadherin staining, with few F-actin stress fibers extending across the cell (Figure 4). In contrast, LT-treated cells showed a marked reduction of peripheral F-actin staining at the intercellular junctions concomitant with a dramatic increase in central stress fibers spanning the length of the cell (Figure 4K). This F-actin redistribution pattern correlated with the elongated cellular appearance observed by phase contrast. Moreover, LT-treated monolayers showed marked alterations in VE-cadherin with incomplete or dispersed staining at intercellular junctions and an overall reduction in membrane-associated VE-cadherin immunofluorescence (Figure 4L). These morphological and immunofluorescence observations, typically observed in connection with altered endothe-

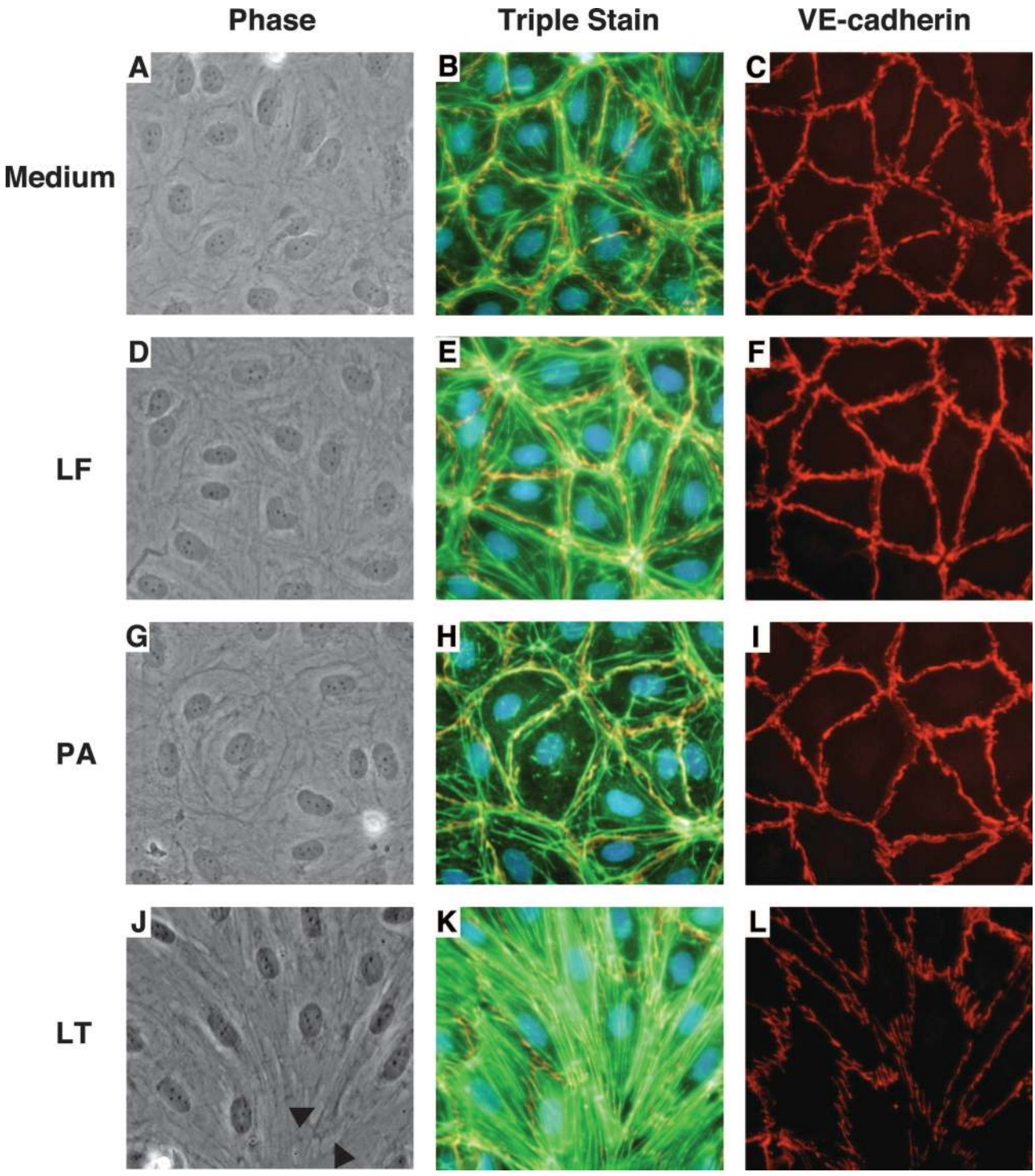

Figure 4. Phase contrast morphology and immunofluorescence visualization of F-actin, VE-cadherin, and nuclei. Cells were incubated with medium alone (**A** to **C**) or medium containing 1 μg/ml LF (**D** to **F**), 1 μg/ml PA (**G** to **I**), or both (**J** to **L**). After 72 hours, monolayers were washed, fixed, and stained with Hoechst 33342 (blue), F-actin (green), and VE-cadherin (red) as described in Materials and Methods. Phase contrast images and corresponding immunofluorescence images were visualized using an inverted microscope (40× objective). LT induced cellular elongation and small interendothelial gaps (**black arrows**) compared with medium, LF, or PA alone. In addition, LT increased central F-actin stress fibers and decreased VE-cadherin immunofluorescence. Images are representative of five separate experiments. Note that in the triple-stained photomicrographs, the VE-cadherin immunofluorescence was masked by the bright F-actin staining.

lial barrier properties, correlated with the changes in TEER and FITC-HSA permeability. To quantitate the apparent loss of membrane-associated VE-cadherin, a cell-based ELISA assay was used (Figure 5). LT induced a significant reduction in the level of cell surface VE-cadherin in endothelial monolayers (~25%, $P < 0.001$). No changes in VE-cadherin were observed with LF or PA alone.

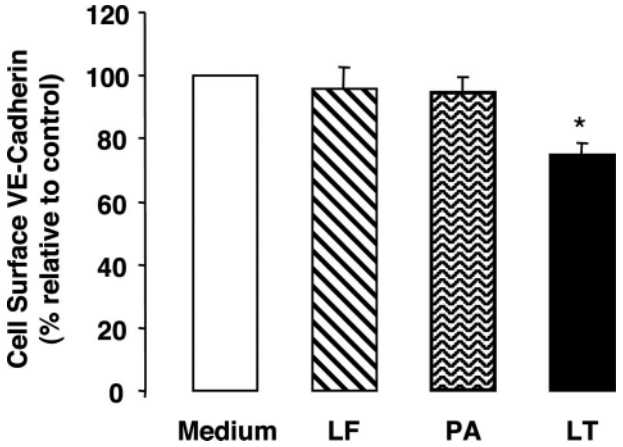

Figure 5. LT decreases cell surface VE-cadherin. Cells were incubated with medium alone or medium containing 1 μg/ml LF, 1 μg/ml PA, or both. After 72 hours, monolayers were washed and fixed in 1% paraformaldehyde. A cell-based ELISA was performed as described in Materials and Methods. Cell surface VE-cadherin was measured as the absorbance at 450 nm. Values were calculated as the percent relative to control and are shown as the means ± SE for a minimum of three independent experiments (n = 3–4). *$P < 0.001$ versus medium alone.

Influence of Monolayer Cell Density and Cell Death on LT-Induced Barrier Dysfunction

Given that LT caused a slight elevation in the nonadherent cell population over the course of 72 hours, we examined whether changes in monolayer cell density or endothelial cell death could account for the observed barrier dysfunction. To assess monolayer cell density, cultures were stained with Hoechst 33342 and PI for the identification and enumeration of adherent cells with normal nuclear morphology while excluding apoptotic and necrotic cells. Through this approach, we also visually determined that LT does not cause direct necrosis as reported for certain cell lines.[2,31] Furthermore, PI-positive cells were generally nonadherent cells with condensed or fragmented nuclei suggesting death via apoptosis. After 12 or 24 hours, LT (1 μg/ml LF and PA) did not cause any change in monolayer density compared with untreated cultures (Figure 6A). After 48 and 72 hours, LT produced a 7 and 12% decrease, respectively, in monolayer density (Figure 6A). LF or PA alone did not produce any change in monolayer density (Figure 6B). LF concentrations of 10 and 100 ng/ml in the presence of 1 μg/ml PA also induced a minor decrease in monolayer density after 72 hours (P = 0.08 and P = 0.13, respectively) (Figure 6B). These minor changes in monolayer cell density as well as the decrease in TEER measured as early as 12 hours (Figure 1) do not support a major role for altered monolayer cell density in the observed barrier dysfunction.

To further assess the potential contribution of LT-mediated cell death in barrier dysfunction, adherent and nonadherent cells were collected and analyzed for apoptosis and/or necrosis using the annexin V/PI assay. Annexin V was used to detect externalized phosphatidylserine (PS) on the outer leaflet of the plasma membrane, an early feature of apoptotic cells. PI uptake served as an index of cells with decreased plasma membrane integrity

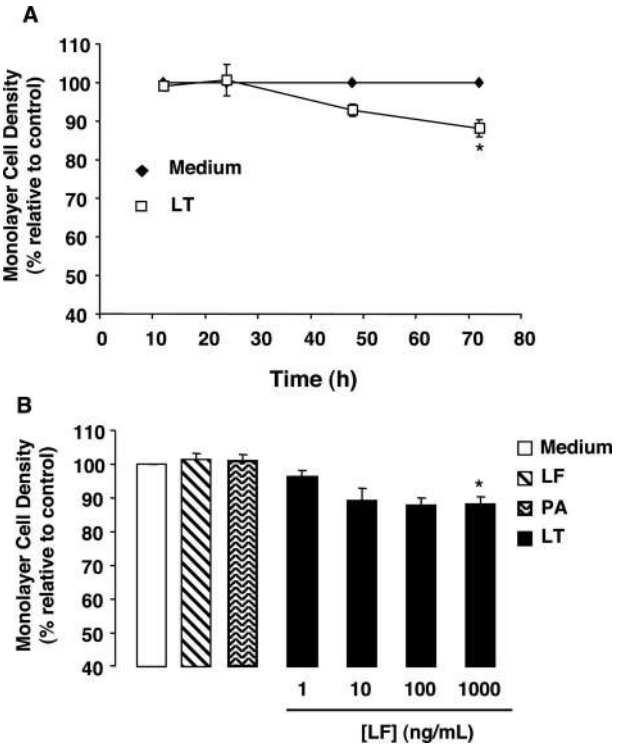

Figure 6. Effect of LT on monolayer cell density. **A:** Confluent cultures in 12- or 24-well dishes were treated with medium alone or medium containing 1 μg/ml LF and 1 μg/ml PA. At the indicated time points, monolayers were stained with Hoechst 33342 and PI. For each treatment, immunofluorescence images of five separate fields were visualized using an inverted microscope (20× objective). For each image, adherent cells with normal nuclear morphology excluding apoptotic and necrotic cells were identified and counted, and the average was tabulated for each well. Monolayer cell density was calculated as the percentage of normal adherent nuclei relative to untreated control wells, and values are reported as the mean ± SE for a minimum of three independent experiments (n = 3 - 6). *$P < 0.05$ versus medium alone. **B:** After 72 hours, monolayer cell density was analyzed after treatment with medium alone, 1 μg/ml LF, 1 μg/ml PA, or varying amounts of LF and 1 μg/ml PA. *$P < 0.05$ versus medium alone (n = 3–6).

indicative of late apoptosis or necrosis. LF or PA alone did not induce cell death at any time interval (Figure 7A). In contrast, LT (1 μg/ml LF and PA) produced a small but significant increase in early apoptotic cells at 48 (2.5%) and 72 hours (7%), but not at 24 hours (Figure 7A). LT also induced a small but significant increase in PI-positive cells at 72 hours (LT, 17 ± 2% versus medium, 12 ± 2%; $P < 0.01$), but not at 24 hours (LT, 8 ± 1% versus medium, 9 ± 1%) or 48 hours (LT, 9 ± 2% versus medium, 8 ± 2%). Figure 7B shows that LT-induced apoptosis was LF concentration dependent with statistically significant increases at 10, 100, and 1000 ng/ml LF in the presence of 1 μg/ml PA. The minor increases in cell death were consistent with the time- and concentration-dependent effects of LT on monolayer cell density (Figure 6) as well as the slight elevations in the nonadherent cell population observed by phase contrast microscopy. However, the onset time and low level of LT-induced apoptosis and necrosis do not support a major role for LT-mediated cell death in the observed barrier dysfunction.

To further rule out LT-induced cell death as a mechanism for barrier dysfunction, we examined the effect of

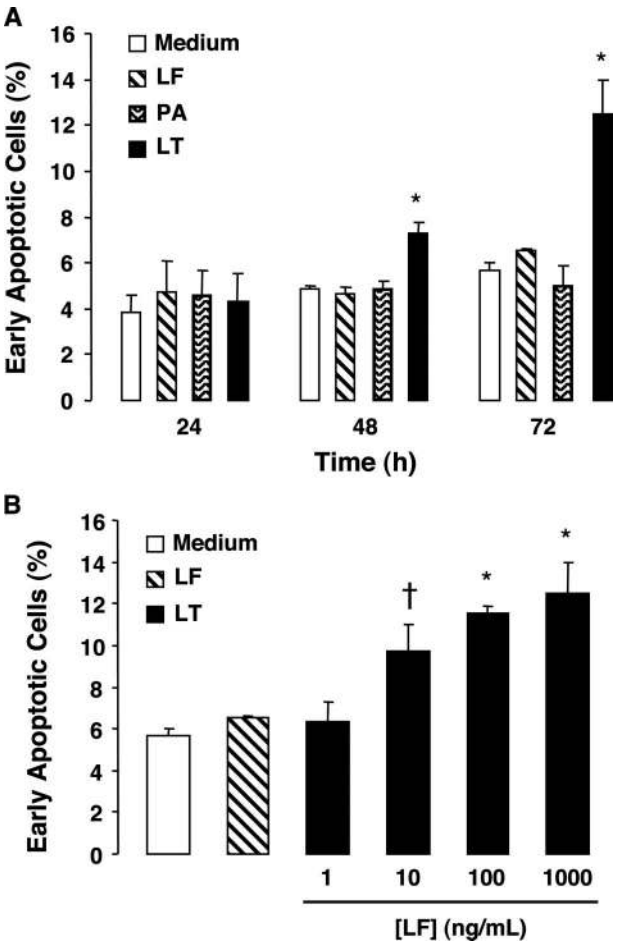

Figure 7. Effect of LT on endothelial apoptosis. **A:** Cells were incubated with medium alone or medium containing 1 μg/ml LF, 1 μg/ml PA, or both (LT). At the indicated time points, PS externalization was measured as described in Materials and Methods. The percentage of early apoptotic cells (annexin V+, PI−) is shown as the means ± SE for a minimum of three independent experiments (n = 3–5). *$P < 0.01$ versus medium alone. **B:** Cells were treated with medium alone, 1 μg/ml LF, or varying amounts of LF in the presence of 1 μg/ml PA. After 72 hours, adherent and nonadherent cells were pooled and analyzed for PS externalization. The percentage of early apoptotic cells (annexin V+, PI−) is shown as the means ± SE for a minimum of three independent experiments (n = 3–5). *$P < 0.01$, †$P < 0.05$ versus medium alone.

zVAD, a general caspase inhibitor. Figure 8A shows that pretreatment with zVAD completely blocked LT-induced apoptosis, confirming the role of caspase activation in apoptotic induction. The basal level of apoptosis in control cultures was also reduced by zVAD. Consistent with the inhibition of apoptosis, zVAD prevented the LT-mediated increase in the PI-positive population (LT, 17% versus LT + zVAD, 10% versus medium, 12%) and the decrease in monolayer density (LT, 88% versus LT + zVAD, 110% relative to untreated cells) after 72 hours. Next, we analyzed F-actin and VE-cadherin distribution by immunofluorescence microscopy. Figure 8B shows that cells treated with zVAD assumed morphology similar to that of untreated cells with peripheral F-actin colocalized with strong intercellular VE-cadherin staining. In contrast, cells treated with LT and zVAD showed remarkable elongation with central stress fibers and altered VE-cadherin distribution, consistent with the changes induced by LT alone (Figure 4). The effect of zVAD on LT-induced barrier dysfunction was also examined. Figure 8C shows that zVAD alone produced a small increase in TEER relative to untreated cells. Interestingly, cells treated with LT and zVAD showed a nearly identical reduction in TEER relative to LT-treated cells, with no significant differences between the two treatments at any time point (Figure 8C). The reduction in TEER also correlated with a similar degree of albumin leakage between LT and LT/zVAD-treated monolayers (Figure 8D). Taken together, these data indicate that LT-induced barrier dysfunction was not dependent on LT-mediated cell death or changes in monolayer cell density.

Effect of LT on Cell Redox Activity

Experiments were also carried out to investigate the possible relationship between LT-induced barrier dysfunction and alterations in cellular metabolic activity as measured by the bioreducing capacity of endothelial monolayers. LF or PA alone did not alter cell redox activity at any time point (data not shown). However, treatment with 1 μg/ml LF and PA significantly decreased MTS reduction at 12 hours (76 ± 5% of control), 24 hours (71 ± 5%), 48 hours (78 ± 5%), and 72 hours (59 ± 3%) (n = 3–5). In addition, cultures treated with 1, 10, and 100 ng/ml LF in the presence of 1 μg/ml PA showed MTS conversions of 89 ± 5%, 63 ± 4%, and 55 ± 3%, respectively, after 72 hours. Given the comparatively minor changes in cell death and monolayer cell density (Figures 6 and 7), these data indicate that LT alters metabolic processes possibly at the level of cell respiration without triggering extensive apoptosis or necrosis. At 12 or 24 hours, for example, LT caused a ~25 to 30% decrease in MTS conversion without any detectable effect on cell death or monolayer cell density. The LF-concentration-dependent inhibition of cell redox activity and its detection as early as 12 hours suggest a possible link between LT-mediated metabolic alterations and the observed barrier dysfunction.

Effect of MEK and MAPK Inhibitors on Barrier Function

Once translocated into cells, LF has been shown to disrupt the activation of the MAPK pathways ERK1/2, p38, and JNK by cleaving upstream activator MEKs 1 through 7, except MEK 5.[2,6–8] Previous studies have shown that the actions of LT on other cell types can be mimicked by treating cells with MEK and MAPK inhibitors.[31–33] To examine whether inhibiting MAPK pathways can modulate barrier function in this cell culture system, cells were treated with U0126, SB203580, or SP600125 individually or with a cocktail of all three inhibitors. U0126 is a highly potent inhibitor of MEK1/2 (upstream activator of ERK1/2), whereas SB203580 and SP600125 are potent inhibitors of p38 and JNK, respectively. Treatment with U0126 and SP600125 produced a 20 and 40% reduction, respectively, in TEER that persisted over the course of 72 hours (Figure 9A). This reduction in TEER correlated with

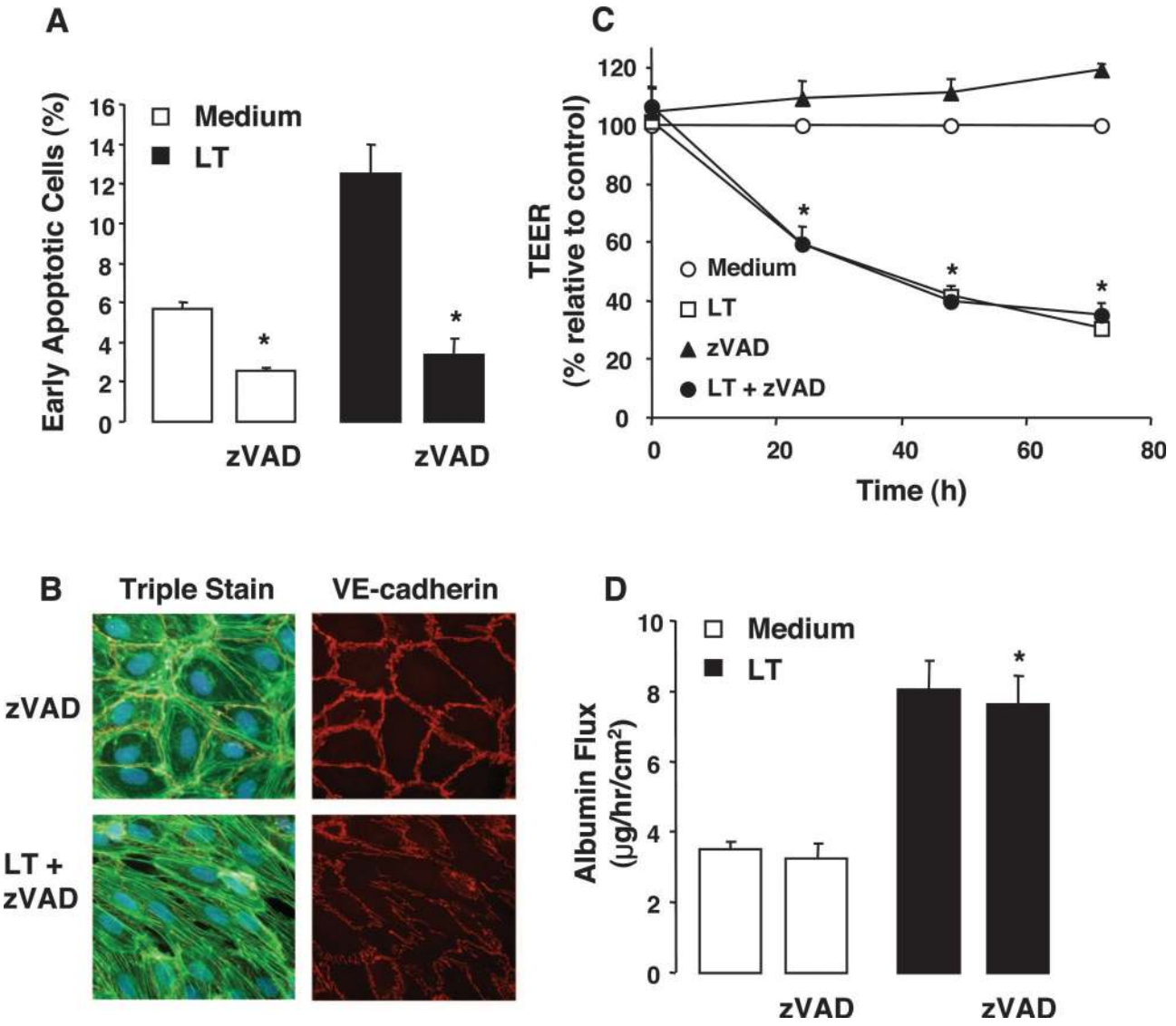

Figure 8. Effect of caspase inhibition on LT-mediated apoptosis and barrier dysfunction. Cells were treated with the general caspase inhibitor, zVAD (80 μmol/L), 1 hour before the addition of 1 μg/ml each of LF and PA. **A:** After 72 hours, adherent and nonadherent cells were pooled and analyzed for PS externalization as described in Materials and Methods. The percentage of early apoptotic cells (annexin V+, PI-) is shown as the means ± SE for a minimum of three independent experiments (n = 3–5). *$P < 0.01$ versus medium alone or LT. There was no significant difference between the two zVAD treatment groups. **B:** After 72 hours, monolayers were washed, fixed, and stained with Hoechst 33342 (blue), F-actin (green), and VE-cadherin (red) as described in Materials and Methods. Immunofluorescence images were visualized as described in Figure 4. **C:** TEER readings were obtained at 0, 24, 48, and 72 hours. Values were reported as the percentage of basal TEER obtained by dividing the resistance values of each treated monolayer by the resistance value of the control monolayer at each given time point. The means ± SE for a minimum of three independent experiments are shown. *$P < 0.01$, LT + zVAD versus zVAD alone. **D:** After 72 hours, the permeability of monolayers to FITC-HSA was measured. Values were calculated as the micrograms of FITC-HSA per hour per square centimeter and reported as the means ± SE for a minimum of three independent experiments. *$P < 0.01$ versus zVAD alone.

small but significant U0126- and SP600125-mediated increases in albumin flux (Figure 9B). Treatment with SB203580 produced a gradual increase in TEER that peaked by 48 hours and a nonsignificant decrease in albumin flux (P = 0.08). The triple inhibitor cocktail did not produce any significant changes in TEER or albumin flux. These data suggest that individual inhibitors of MAPK pathways can modulate basal barrier function. However, the triple inhibitor cocktail, which would presumably most closely mimic the effects of LT on MAPK pathways, did not alter barrier function.

Discussion

These findings demonstrate that LT causes barrier dysfunction in cultured human endothelial monolayers, providing a possible link between LT and the prominent vascular leakage associated with systemic anthrax infection in humans and nonhuman primates.[18–23] In the present study, LT-induced barrier dysfunction was prominently observed 2 to 3 days after LT treatment. Interestingly, purified LT injections in mice produced vascular leakage and death over a comparable time course.[11]

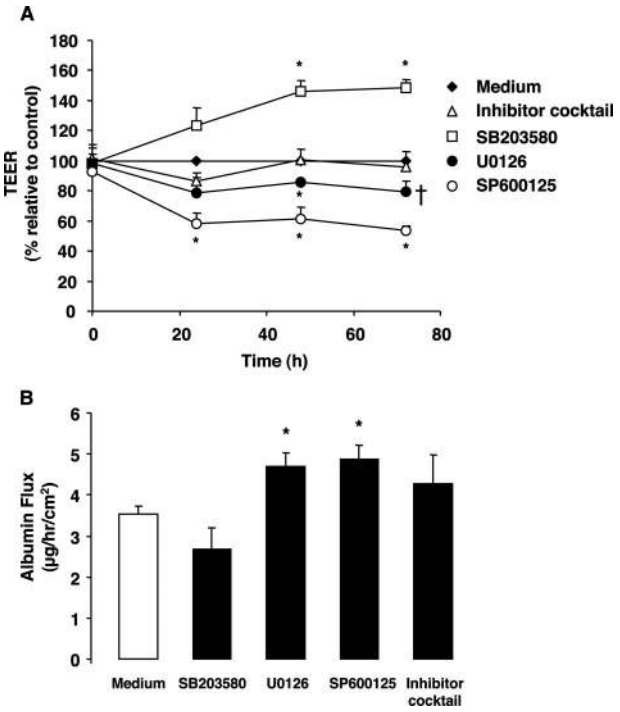

Figure 9. Effect of MEK and MAP kinase inhibitors on barrier function. Cells were treated with 10 μmol/L U0126 (MEK1/2 inhibitor), 10 μmol/L SP600125 (JNK inhibitor), or 20 μmol/L SB203580 (p38 inhibitor) individually or with the inhibitor cocktail (the combination of all three inhibitors). **A:** TEER readings were measured at the indicated time intervals and reported as the means ± SE for a minimum of three independent experiments. $^{*}P < 0.01$, $^{\dagger}P < 0.05$ versus medium alone. **B:** Monolayer permeability to FITC-HSA after 72 hours. Values were calculated as the micrograms of FITC-HSA per hour per square centimeter and reported as the means ± SE for a minimum of three independent experiments. $^{*}P < 0.05$ versus medium alone.

Clinical presentation of anthrax patients suggests a similarly progressive pathogenesis with increasing pleural effusions and hemorrhages observed 3 to 5 days after the onset of initial symptoms.[19] In some reported cases, pleural effusions and hemorrhages occurred despite effective antibiotic treatment, providing support for the important pathogenic role of the toxin.[18] Our *in vitro* findings suggest that the molecular events underlying LT-induced barrier dysfunction implicate the progressive rearrangement of the actin cytoskeleton and altered VE-cadherin distribution in adherens junctions. However, the exact molecular target(s) or pathway(s) altered by LT that subsequently trigger barrier dysfunction is not yet known.

In vascular endothelium, AJs play a central role in regulating barrier function by maintaining intercellular contacts and monolayer integrity. VE-cadherin, the main component of adherens junctions, mediates calcium-dependent homophillic binding and adhesion between endothelial cells. Increased vascular permeability observed in animals after the injection of monoclonal VE-cadherin antibodies supports the important role of VE-cadherin in barrier function regulation *in vivo*.[24] In quiescent endothelium, AJs are anchored to the actin cytoskeleton, which is predominantly clustered around the periphery of the cell. Similar to the LT-induced changes in the present study, increased monolayer permeability induced by cytokines, growth factors, oxidative stress, and toxins is typically accompanied by altered VE-cadherin distribution and rearrangement of the F-actin from a peripheral bundle to *trans*-cellular stress fibers.[27,28] A multitude of signaling pathways have been implicated in the regulation of barrier function.[34,35] In particular, MAPK activation mediates the increased vascular permeability produced by inflammatory mediators (eg, histamine), tumor necrosis factor-α, vascular endothelial growth factor, and oxidative stress.[34] In this context, the finding that LT increases monolayer permeability is somewhat paradoxical given that LT has been shown to inhibit MAPK signaling in several different cell types, including endothelial cells.[6–8] LT cleaves MEK 1 through 7 (except MEK 5), thus disrupting the ERK 1/2, JNK, and p38 pathways. Our studies with chemical MEK and MAPK inhibitors suggest that modulating individual MAPK pathways can alter basal barrier function (Figure 9). However, the triple inhibitor cocktail failed to produce barrier dysfunction. Moreover, we found that neither the individual inhibitors nor the cocktail reproduced the morphological features induced by LT over the course of 3 days. Thus, these observations suggest that the mechanisms underlying the SP600125- or U0126-induced barrier dysfunction may differ from those involved in the LT-mediated barrier dysfunction. Our present findings, therefore, only casually support a role for altered MAPK signaling in LT-induced barrier dysfunction. Given the complex interplay between MAPK pathways and the possible contribution of other signaling pathways, further studies will be required to delineate the mechanisms underlying this LT-mediated phenomenon.

A previous study reported that LT induces apoptosis of human umbilical vein endothelial cells.[8] We found that high amounts of LT induced only minor increases in apoptosis and/or necrosis in confluent primary human lung microvascular endothelial cell cultures. Furthermore, our zVAD inhibitor experiments provide convincing evidence that LT-mediated barrier dysfunction was not dependent on the minor changes in endothelial cell death or monolayer cell density (Figure 8). Several factors could account for the differences between our study and the previous study[8] including the different cell types, culture media, passage number, source of toxin, or the state of confluence prior to toxin treatment. However, it is interesting to note that widespread endothelial injury was not observed in LT-treated mice or rats that developed vascular leakage.[11,12] Furthermore, to the best of our knowledge, endothelial apoptosis has not been a common finding in clinical cases or experimental models of inhalational anthrax.

Previous studies also reported that LT inhibited cell redox activity in human umbilical vein endothelial cells.[8,36] In the present study, we found that the addition of LT (≥10 ng/ml LF and 1 μg/ml PA) to confluent endothelial cultures decreased cell redox activity by ~40% over the course of 3 days. These results correlate well with the results of Pandey and Warburton,[36] but not those of Kirby (>90% after 3 days).[8] Other markers of LT-mediated cell death were not evaluated in the Pandey and Warburton study, whereas the Kirby study related these data to apoptosis and/or necrosis. In our study, LT caused only minor changes in apoptosis, necrosis, and

monolayer cell density, therefore we interpret the decrease in the ability to convert MTS as being indicative of a LT-mediated inhibition of cellular metabolic activity. The exact nature of these metabolic disturbances and the possible link to changes in endothelial morphology and barrier function is the subject of current studies in our laboratory.

Further investigation of the molecular events leading to LT-induced barrier dysfunction will clarify the potential link with altered MAPK signaling events or possibly lead to the identification of new targets for LT. Understanding how LT disrupts the vasculature could provide insight on how to manage the later stages of an established anthrax infection. This knowledge may be useful in developing vascular-targeted therapies to delay the rapid progression of the disease and improve the therapeutic window for treating the existing bacteremia and toxemia.

Acknowledgments

We thank Dr. S.H. Leppla and Dr. M. Moayeri (National Institute of Allergy and Infectious Diseases, National Institutes of Health) for helpful discussions and critical reading of the manuscript. We also thank Dr. Leppla for kindly providing the anthrax toxin proteins.

References

1. Leppla SH: The bifactorial Bacillus anthracis lethal and oedema toxins. Comprehensive Sourcebook of Bacterial Protein Toxins. Edited by JA Alouf, J Freer. London, Academic Press, 1999, pp 243–263
2. Moayeri M, Leppla SH: The roles of anthrax toxin in pathogenesis. Curr Opin Microbiol 2004, 7:19–24
3. Mock M, Fouet A: Anthrax. Annu Rev Microbiol 2001, 55:647–671
4. Bradley KA, Mogridge J, Mourez M, Collier RJ, Young JA: Identification of the cellular receptor for anthrax toxin. Nature 2001, 414:225–229
5. Scobie HM, Rainey GJ, Bradley KA, Young JA: Human capillary morphogenesis protein 2 functions as an anthrax toxin receptor. Proc Natl Acad Sci USA 2003, 100:5170–5174
6. Bardwell AJ, Abdollahi M, Bardwell L: Anthrax lethal factor-cleavage products of mitogen-activated protein kinase (MAPK) kinases exhibit reduced binding to their cognate MAPKs. Biochem J 2004, 378:569–577
7. Duesbery NS, Webb CP, Leppla SH, Gordon VM, Klimpel KR, Copeland TD, Ahn NG, Oskarsson MK, Fukasawa K, Paull KD, Vande Woude GF: Proteolytic inactivation of MAP-kinase-kinase by anthrax lethal factor. Science 1998, 280:734–737
8. Kirby JE: Anthrax lethal toxin induces human endothelial cell apoptosis. Infect Immun 2004, 72:430–439
9. Leppla SH: Anthrax toxin edema factor: a bacterial adenylate cyclase that increases cyclic AMP concentration in eukaryotic cells. Proc Natl Acad Sci USA 1982, 79:3162–3166
10. Ulmer TS, Soelaiman S, Li S, Klee CB, Tang WJ, Bax A: Calcium dependence of the interaction between calmodulin and anthrax edema factor. J Biol Chem 2003, 278:29261–29266
11. Moayeri M, Haines D, Young HA, Leppla SH: Bacillus anthracis lethal toxin induces TNF-α-independent hypoxia-mediated toxicity in mice. J Clin Invest 2003, 112:670–682
12. Cui X, Moayeri M, Li Y, Li X, Haley M, Fitz Y, Correa-Araujo R, Banks SM, Leppla SH, Eichacker PQ: Lethality during continuous anthrax lethal toxin infusion is associated with circulatory shock but not inflammatory cytokine or nitric oxide release in rats. Am J Physiol Regul Integr Comp Physiol 2004, 286:R699–R709
13. Ezzell JW, Ivins BE, Leppla SH: Immunoelectrophoretic analysis, toxicity, and kinetics of in vitro production of the protective antigen and lethal factor components of Bacillus anthracis toxin. Infect Immun 1984, 45:761–767
14. Pezard C, Berche P, Mock M: Contribution of individual toxin components to virulence of Bacillus anthracis. Infect Immun 1991, 59:3472–3477
15. Beall FA, Dalldorf FG: The pathogenesis of the lethal effect of anthrax toxin in the rat. J Infect Dis 1966, 116:377–389
16. Dalldorf FG, Beall FA: Capillary thrombosis as a cause of death in experimental anthrax. Arch Pathol 1967, 83:154–161
17. Smith H, Stoner HB: Anthrax Toxic Complex. Fed Proc 1967, 26:1554–1557
18. Guarner J, Jernigan JA, Shieh WJ, Tatti K, Flannagan LM, Stephens DS, Popovic T, Ashford DA, Perkins BA, Zaki SR: Inhalational Anthrax Pathology Working Group: pathology and pathogenesis of bioterrorism-related inhalational anthrax. Am J Pathol 2003, 163:701–709
19. Plotkin SA, Brachman PS, Utell M, Bumford FH, Atchison MM: An epidemic of inhalational anthrax, the first in the twentieth century: I. Clinical features. Am J Med 2002, 112:4–12
20. Grinberg LM, Abramova FA, Yampolskaya OV, Walker DH, Smith JH: Quantitative pathology of inhalational anthrax. I: quantitative microscopic findings. Mod Pathol 2001, 14:482–495
21. Vasconcelos D, Barnewall R, Babin M, Hunt R, Estep J, Nielsen C, Carnes R, Carney J: Pathology of inhalation anthrax in cynomolgus monkeys (Macaca fascicularis). Lab Invest 2003, 83:1201–1209
22. Fritz DL, Jaax NK, Lawrence WB, Davis KJ, Pitt ML, Ezzell JW, Friedlander AM: Pathology of experimental inhalation anthrax in the rhesus monkey. Lab Invest 1995, 73:691–702
23. Leendertz FH, Ellerbrok H, Boesch C, Couacy-Hymann E, Matz-Rensing K, Hakenbeck R, Bergmann C, Abaza P, Junglen S, Moebius Y, Vigilant L, Formenty P, Pauli G: Anthrax kills wild chimpanzees in a tropical rainforest. Nature 2004, 430:451–452
24. Gotsch U, Borges E, Bosse R, Boggemeyer E, Simon M, Mossmann H, Vestweber D: VE-cadherin antibody accelerates neutrophil recruitment in vivo. J Cell Sci 1997, 110:583–588
25. Hordijk PL, Anthony E, Mul FP, Rientsma R, Oomen LC, Roos D: Vascular-endothelial-cadherin modulates endothelial monolayer permeability. J Cell Sci 1999, 112:1915–1923
26. Dudek SM, Garcia JGN: Cytoskeletal regulation of pulmonary vascular permeability. J Appl Physiol 2001, 91:1487–1500
27. Vincent PA, Xiao K, Buckley KM, Kowalczyk AP: VE-cadherin: adhesion at arm's length. Am J Physiol Cell Physiol 2004, 286:C987–C997
28. Dejana E, Bazzoni G, Lampugnani MG: Vascular endothelial (VE)-cadherin: only an intercellular glue? Exp Cell Res 1999, 252:13–19
29. Park S, Leppla SH: Optimized production and purification of Bacillus anthracis lethal factor. Protein Expr Purif 2000, 18:293–302
30. Ramirez DM, Leppla SH, Schneerson R, Shiloach J: Production, recovery and immunogenicity of the protective antigen from a recombinant strain of Bacillus anthracis. J Ind Microbiol Biotechnol 2002, 28:232–238
31. Kim SO, Jing Q, Hoebe K, Beutler B, Duesbery NS, Han J: Sensitizing anthrax lethal toxin-resistant macrophages to lethal toxin-induced killing by tumor necrosis factor-alpha. J Biol Chem 2003, 278:7413–7421
32. Webster JI, Tonelli LH, Moayeri M, Simons SS Jr, Leppla SH, Sternberg EM: Anthrax lethal factor represses glucocorticoid and progesterone receptor activity. Proc Natl Acad Sci USA 2003, 100:5706–5711
33. Agrawal A, Lingappa J, Leppla SH, Agrawal S, Jabbar A, Quinn C, Pulendran B: Impairment of dendritic cells and adaptive immunity by anthrax lethal toxin. Nature 2003, 424:329–334
34. Bogatcheva NV, Dudek SM, Garcia JG, Verin AD: Mitogen-activated protein kinases in endothelial pathophysiology. J Investig Med 2003, 51:341–352
35. Yuan SY: Protein kinase signaling in the modulation of microvascular permeability. Vascul Pharmacol 2002, 39:213–223
36. Pandey J, Warburton D: Knock-on effect of anthrax lethal toxin on macrophages potentiates cytotoxicity to endothelial cells. Microbes Infect 2004, 6:835–843